HAL
open science

Simulation of Na D emission near Europa during eclipse

T. A. Cassidy, R. E. E. Johnson, P. E. Geissler, François Leblanc

To cite this version:

T. A. Cassidy, R. E. E. Johnson, P. E. Geissler, François Leblanc. Simulation of Na D emission near Europa during eclipse. Journal of Geophysical Research. Planets, 2008, 113 (E2), pp.E02005. 10.1029/2007JE002955 . hal-00256762

HAL Id: hal-00256762

https://hal.science/hal-00256762v1

Submitted on 7 Feb 2016

HAL is a multi-disciplinary open access archive for the deposit and dissemination of scientific research documents, whether they are published or not. The documents may come from teaching and research institutions in France or abroad, or from public or private research centers.

L'archive ouverte pluridisciplinaire **HAL**, est destinée au dépôt et à la diffusion de documents scientifiques de niveau recherche, publiés ou non, émanant des établissements d'enseignement et de recherche français ou étrangers, des laboratoires publics ou privés.

Simulation of Na *D* emission near Europa during eclipse

T. A. Cassidy,[1] R. E. Johnson,[1] P. E. Geissler,[2] and F. Leblanc[3,4]

Received 15 June 2007; revised 20 October 2007; accepted 30 November 2007; published 14 February 2008.

[1] The Cassini imaging science subsystem observed Europa in eclipse during Cassini's Jupiter flyby. The disk-resolved observations revealed a spatially nonuniform emission in the wavelength range of 200–1050 nm (clear filters). By building on observations and simulations of Europa's Na atmosphere and torus we find that electron-excited Na in Europa's tenuous atmosphere can account for the observed emission if the Na is ejected preferentially from Europa's dark terrain.

Citation: Cassidy, T. A., R. E. Johnson, P. E. Geissler, and F. Leblanc (2008), Simulation of Na *D* emission near Europa during eclipse, *J. Geophys. Res.*, *113*, E02005, doi:10.1029/2007JE002955.

1. Introduction

[2] Jupiter's moon Europa is exposed to ion, electron, and photon flux that erodes the surface, launching atoms and molecules into ballistic trajectories to form a tenuous atmosphere [e.g., *Johnson et al.*, 2004]. One component of that atmosphere is neutral atomic sodium, which has been observed by ground-based telescopes [e.g., *Leblanc et al.*, 2005]. Those observations and models focused on the gravitationally unbound component of the sodium atmosphere, which forms a Jupiter-orbiting neutral cloud near Europa's orbit [*Burger and Johnson*, 2004]. This cloud is made visible by sodium's efficient scattering of sunlight. In this paper we present a model of observations of Europa's near-surface atmosphere (within hundreds of kilometers of the surface) taken while Europa was in eclipse. The observations were performed by the Cassini spacecraft imaging science subsystem (ISS) during Cassini's Jupiter flyby. The ISS narrow angle camera (NAC) revealed emissions (Figures 1a and 1b) that, because of the absence of sunlight, could only have been produced by an auroral process, i.e., ion and electron impact excitation of the atmosphere. What was particularly interesting is that the emissions were brightest in a quadrant opposite to where the oxygen emissions were brightest [*Cassidy et al.*, 2007; *McGrath et al.*, 2004].

[3] Figure 1a was reproduced from *Porco et al.* [2003, supporting online material]. It shows the first 5 of 15 observations during which Europa entered eclipse. Europa is fully in eclipse by the second observation. The observations in Figure 1b are averages of later images and have had reflected sunlight from Ganymede removed. This was done by assuming that Europa has a Minnaert coefficient of 0.65 and a uniform albedo. Fixed pattern noise was removed with a Fourier filter. Figure 1b (left) shows the average of the last 5 observations, and Figure 1b (right) shows the average of the last 9 observations. That these images are nearly identical indicates a lack of variability deep into the eclipse. In both cases the peak brightness was on the order of 10 kR. The noise is on the order of 5 kR.

[4] The eclipse observations were performed with one of two filter settings, two clear filters and another set that looked for O emissions. The clear filters, CL1 and CL2, provide sensitivity to the wavelength range 200–1050 nm, with maximum sensitivity at 611 nm [*Porco et al.*, 2004]. Within that wavelength range, there are a number of lines that might contribute to the observed glow. These include the electron impact-induced excitation of Na [*Kim*, 2001], O [*Smyth and Marconi*, 2000, Figure 4], O_2, K [*Johnson et al.*, 2002], SO_2 [*Ajello et al.*, 1992], and Mg. Ion-induced excitation may also make a small contribution to these processes [e.g., *Allen et al.*, 1988]. Of these, the Na *D* line (~589 nm) is likely the dominant emission in eclipse, as Na is relatively abundant and easily excited. Of the other species, Mg, K, and O_2 are likely the brightest. K is on the order of ~1/10 the brightness of Na, since the K column density is about 1/25 that of Na [*Brown*, 2001; *Johnson et al.*, 2002] and its cross section for electron impact excitation is about twice that of Na [*Kim*, 2001]. The electron impact dissociation of O_2 produces visible emissions from atomic oxygen in addition to the well-known UV emissions at 130.4 and 135.6 nm. On the basis of what is known of the O_2 atmosphere [*Hall et al.*, 1998; *Cassidy et al.*, 2007] the visible emissions should be on the same order of magnitude as the UV, 100 R, mostly at 777.4 and 844.6 nm [*Zipf et al.*, 1978; *Kanik et al.*, 2003].

[5] The ultimate origin of sodium is uncertain, but hydrates such as Na_2SO_4 or $MgSO_4$ have been suggested [*Zolotov and Shock*, 2001; *Orlando et al.*, 2005]. These hydrated substances are correlated with the dark material in Figure 1c, a visible light image mosaic of Europa's surface from the same perspective as the eclipse observations. That these dark materials are somewhat correlated to the

[1]Engineering Physics Program and Department of Astronomy, University of Virginia, Charlottesville, Virginia, USA.
[2]U.S. Geological Survey, Flagstaff, Arizona, USA.
[3]Service d'Aéronomie du Centre National de la Recherche Scientifique, Verrières-le-Buisson, France.
[4]Osservatorio Astronomico di Trieste, Trieste, Italy.

Copyright 2008 by the American Geophysical Union.
0148-0227/08/2007JE002955

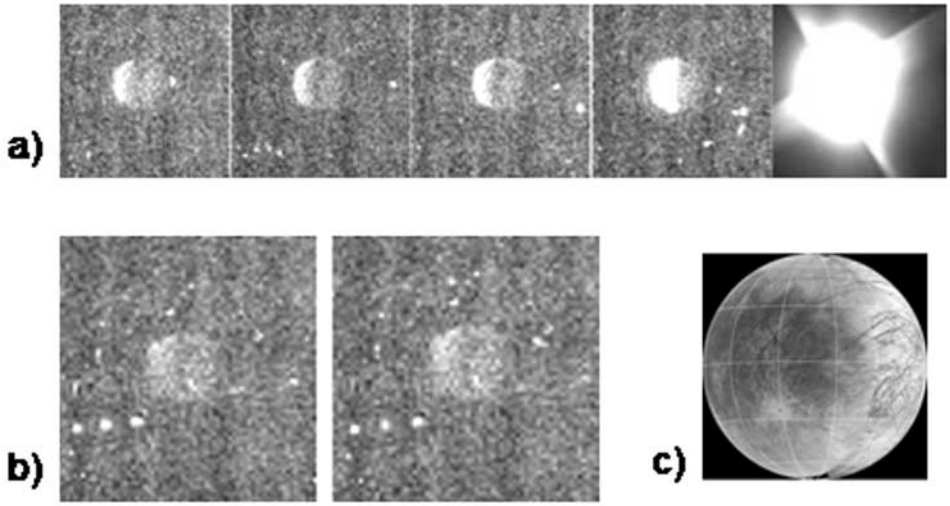

Figure 1. (a) First 5 (out of 15) images of Europa made using the Cassini ISS NAC with clear filters (reproduced from *Porco et al.* [2003]). The first observation is shown in the fifth panel and shows Europa in penumbra. The second image shows Europa in umbra, but there still may be significant contamination by light scattered though Jupiter's atmosphere. The time between images is 5.5 min. (b) Average of later images. The peak brightness is on the order of 10 kR. Reflected light from Ganymede has been removed. (left) Average of the last 5 observations (out of 12); (right) average of the last 9 taken. The observations were taken over 27.5 min in Figure 1b (left) and 49.5 min in Figure 1b (right). (c) A visible light mosaic of Europa's surface from Galileo imagery showing the same perspective as Figures 1a and 1b.

auroral brightness is suggestive of a Na-rich surface and motivated the simulations discussed below.

[6] There are no experimental data for sputtering this hydrate, but the most abundant product from pure Na_2SO_4 is Na [*Wiens et al.*, 1997]. Because sodium is redistributed by sputtering, much of the observed atmospheric sodium is ejected along with the ice matrix [*Leblanc et al.*, 2005]. Assuming that hydrated Mg sulfate is present in the surface in similar abundances and is similarly sputtered, then one might expect a similar column density. However, we do not expect its emissions to appear as bright as Na. The Mg cross section for electron excitation is about half that of Na [*Kim*, 2001], resulting in one half of the photon emission rate at a wavelength of 282.5 nm. Combined with NAC's lower efficiency at detecting the Mg emission wavelength [*Porco et al.*, 2004], the Mg contribution to the signal in Figure 1 is at least an order of magnitude less than Na.

[7] Observations taken to look for O emissions at 630 and 636 nm were interspersed among the clear filters observations (filters CB1 and CL1). The observations revealed nothing above the noise level, which is on the order of 5 kR. This is in agreement with the estimates of *Smyth and Marconi* [2006], who predicted an O intensity at 630 nm of less than 1 R.

2. Model Description

[8] The Na atmosphere simulations reported here were adapted from a Monte Carlo simulation of Europa's O_2 atmosphere [*Cassidy et al.*, 2007]. Simulations were carried out to determine the spatial distribution of the Na atmosphere using about 10^6 test particles. These particles are ejected from the surface using the angular distribution

$$\frac{dP}{d\cos(\theta)} = 2\cos(\theta), \tag{1}$$

where θ is the angle of ejection with respect to the surface normal [*Cassidy and Johnson*, 2005] and P is the probability of emission. The energy distribution of ejected Na was found by assuming that the Na is carried out of the surface with sputtered H_2O molecules [*Johnson*, 2000]. The dominant agents of water ice sputtering at Europa are heavy energetic ions, each of which ejects hundreds of water molecules. Impurities in the ice are carried out along with the sputtered H_2O molecules, and with roughly the same speed or energy distribution as the H_2O molecules, it is uncertain which is appropriate. If impurities have the same speed distribution as sputtered H_2O, then the resulting energy distribution for sputtered Na atoms is given by

$$\frac{dP}{dE} = \frac{2(m/M)^2 EU}{(U + (m/M)E)^3}, \tag{2}$$

where U is 0.055 eV, E is the Na atom energy, m is the mass of a water molecule, and M is the mass of a Na atom. This expression was created from the H_2O energy distribution found by *Reimann et al.* [1984]. Because the mass ratio, m/M, is close to one, this is nearly equivalent to using the same energy distribution as H_2O, which was shown to be consistent with observations of Europa's Na torus [*Leblanc et al.*, 2005]. The simulations by *Leblanc et al.* [2005] suggest that Na ejected by photon-stimulated desorption can

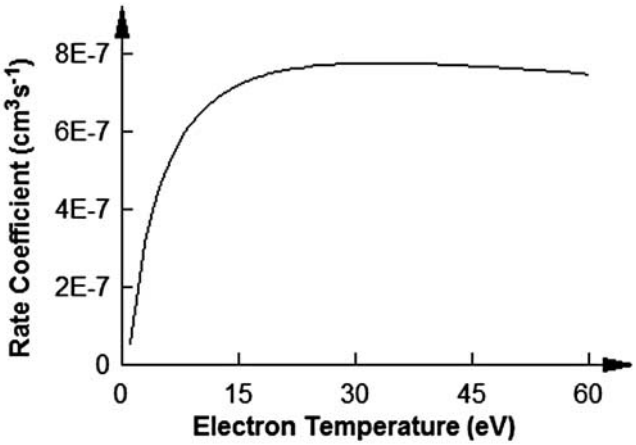

Figure 2. Rate coefficient for electron excitation of Na *D* emission as a function of electron temperature. Multiplying the rate coefficient by electron density yields the frequency at which a Na atom will emit photons.

be important; however, the energy distribution for photon-stimulated desorption is quite similar to equation (2) [*Johnson et al.*, 2002]. Na ejected by electron-stimulated desorption may also contribute to the eclipse observation with a similar energy distribution. Therefore, in our simulations, all of the Na is sputtered using equation (2).

[9] Once the energy and direction are chosen for a test particle, its trajectory is calculated. The Na atmosphere is approximated as ballistic; gravity is the only force on Na in the absence of sunlight. On the basis of our model for the O_2 atmosphere [*Cassidy et al.*, 2007], collisions between Na atoms and other atmospheric components have only a small effect and can be neglected during eclipse. The gravity of Jupiter is also neglected, as, unlike the simulations by *Leblanc et al.* [2005], we are concerned with the near-surface atmosphere (within hundreds of kilometers of the surface) where the Na density is highest.

[10] Sodium has a lifetime against ionization of about 2.0×10^5 s [*Leblanc et al.*, 2005]. We implement this loss process, but since we focus on the near-surface atmosphere, sticking and gravitational escape dominate. Assuming unit sticking efficiency and escape when Na atoms make it to Europa's Hill sphere, the average Na lifetime is about 4500 s.

[11] The trajectories, along with an assumed Na source rate, allow calculation of Na densities [e.g., *Cassidy et al.*, 2007]. Calculating the emission intensity requires an emission rate, which depends on the excitation process. The dominant excitation source in eclipse leading to *D* line emission is electron impact. Collisions with ions can also contribute and have a similar excitation cross section [*Allen et al.*, 1988] but have a much lower flux due to their much lower average speed. The electron environment near Europa was measured by radio occultation [*Kliore et al.*, 1997]. It was found that the electron density falls roughly exponentially with distance from the surface, with a scale height of about 300 km and a surface density of 10^4 cm^{-3}. The measurements were quite noisy, making it difficult to accurately give the variation of density in latitude and longitude, so we will at first assume that the surface electron density is uniform (does not vary with latitude or longitude). *Saur et al.* [1998] predict that the highest density is on the "flanks," (sub- and anti-Jovian hemispheres), along with an electron-free cavity on the leading hemisphere; we will also explore this possibility.

[12] The electron temperature is less certain. The electron temperature at Europa's orbit, but far from its surface, is about 20 eV, and there is a small nonthermal population. *Saur et al.* [1998] predict that the electron density and temperature are anticorrelated, but on the trailing hemisphere, the hemisphere seen by *Porco et al.* [2003], the temperature does not drop below about 19 eV.

[13] Figure 2 shows the rate coefficient for Na *D* (including both *D*1 and *D*2) emission as a function of electron temperature. It was calculated from the cross sections by *Kim* [2001]. The rate coefficient is fairly constant in the temperature range of interest (~10–20 eV). At 20 eV the rate coefficient is 7.5×10^{-7} cm^3 s^{-1}, while at 8 eV, the lowest temperature predicted by *Saur et al.* [1998] for Europa, the rate coefficient is 6.0×10^{-7} cm^3 s^{-1}. Thus electron density is the primary factor in determining the Na *D* emission rate. We neglect variations in temperature and use a constant rate coefficient of 7.0×10^{-7} cm^3 s^{-1} in our simulations.

[14] The Cassini observations in Figure 1 were taken over an hour and began at the beginning of the eclipse. Because of the lifetime mentioned above, some photo-desorbed Na could contribute to the earliest images. However, most of the emission comes from near the surface, where the population has a much shorter lifetime. For instance, the average lifetime of Na atoms that reach 600 km altitude or less (two electron scale heights) is about 400 s. Therefore we assume here that the spatial distribution of Na ejection does not vary in time.

[15] The observations show significant variability up until about 1300 s into the eclipse (Figure 1a) [*Porco et al.*, 2003] even though Europa had entered umbral eclipse by the second image (Figure 1a, fourth panel). In addition to a short-lived population of photo-desorbed Na, this is likely explained by light scattered through Jupiter's atmosphere, which was seen by Cassini observations of Io in eclipse [*Geissler et al.*, 2004].

3. Results

[16] Cassini made several observations of Europa in eclipse. The view is centered 17° east of the trailing hemisphere apex (253°W). The peak brightness, seen on the northern sub-Jovian limb, is on the order of 10 kR.

[17] We explored a variety of sodium ejection scenarios by varying the spatial distribution of Na ejection. In one such distribution [*Leblanc et al.*, 2005, 2002], sodium is emitted preferentially from the trailing hemisphere with a spatial distribution given by

$$\frac{dP}{d\cos(\Theta)} = 1 + 5.5\cos(\Theta)H[\cos(\Theta)], \qquad (3)$$

where Θ is the angle from the trailing hemisphere apex and H is the step function. Equation (3) is an expression for the

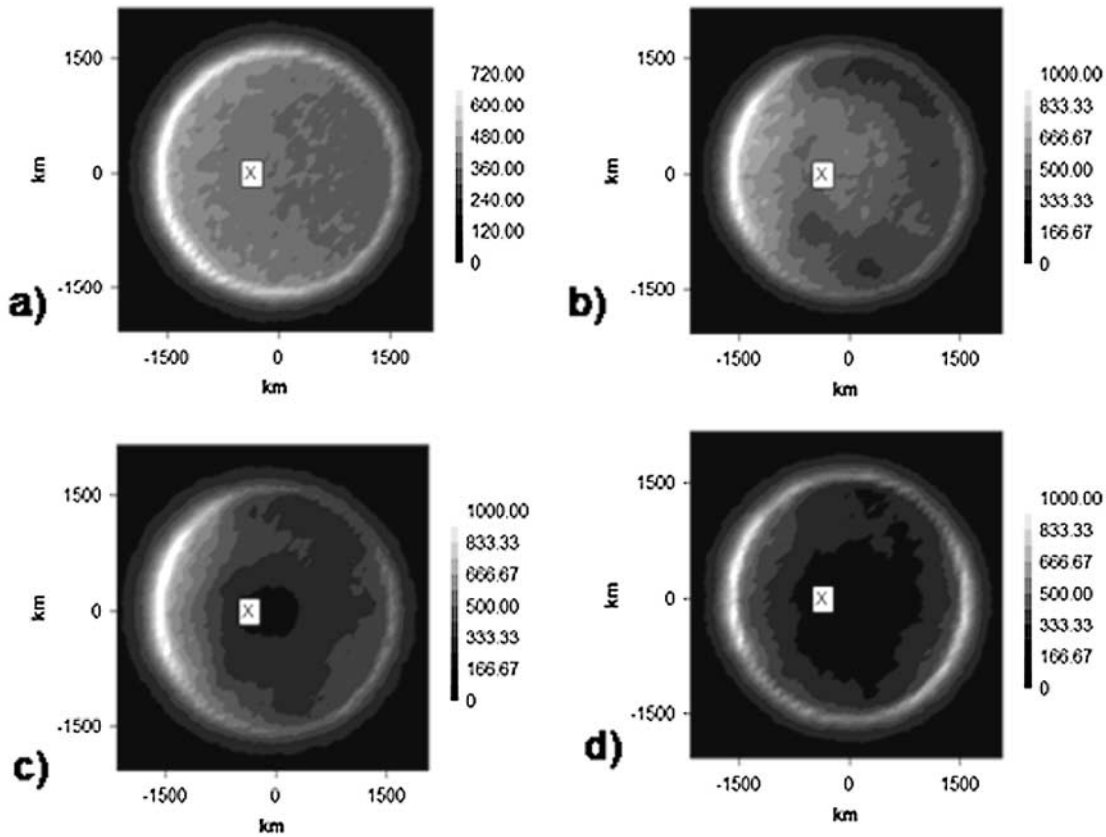

Figure 3. (a) Simulation of case 1. (b) Simulation of case 2. (c) Simulation of case 3. (d) Simulation of case 4. Legends show Na *D* line (~589 nm) emission in rayleighs. The trailing hemisphere apex is marked by cross.

surface's darkness (in the blue end of the visible spectrum) as a function of Θ [*Pospieszalska and Johnson*, 1989; *McEwen*, 1986]. Since surface darkness may be correlated to sodium [*Spencer et al.*, 2006], equation (3) was used as the spatial distribution of Na ejection by *Leblanc et al.* [2005] to reproduce observations of the extended sodium atmosphere at Europa's orbit.

[18] In addition to this global darkness trend, *McEwen* [1986] identified localized regions of dark terrain by removing the global trend of equation (3). We used McEwen's map of localized dark terrain to create another spatial distribution of sodium ejection for use both with and instead of equation (3). Specifically, we had Na ejected from the geological units that McEwen defined as (1) darkest, (2) second darkest, and (3) third darkest, and no emission from the brightest unit, unit 4. We implemented this preferential ejection by multiplying the test particle weight by a coefficient 1 for test particles ejected from the darkest unit, unit 1; 2/3 from unit 2; and 1/3 from unit 3 (while being careful not to affect the total source rate). Despite McEwen's removal of the global trend, these dark regions are also predominantly on the trailing hemisphere. These dark units, including the exogenic contribution, can be seen in Figure 1c.

[19] A simulation of the sodium emission intensity based on equation (3), and without preferential emission from *McEwen*'s [1986] dark units, is shown in Figure 3a and is labeled "case 1" in Table 1. It was made with using latitude- and longitude-independent electron density near the surface. Like the Cassini observations, the simulation is brighter toward the left side of Europa's disk (which includes the trailing hemisphere portion of the sub-Jovian hemisphere) but is otherwise more uniform than the observation. The brightness (in Rayleighs) was calculated using the rate coefficient and electron density described above. The total plasma-induced sputtering rate for Na was set to be 9.3×10^{24} Na s^{-1} by *Leblanc et al.* [2002, 2005]. They reported it as a globally averaged rate of 3×10^{7} Na cm^{-2} s^{-1}. Although the plasma flux may vary by up to a factor of 5 [*Paranicas et al.*, 2002], we will use the above rate for all simulations in this paper. We explore other spatial distributions for Na ejection below, but the total source rate is kept constant.

[20] For case 2 we included, in addition to preferential ejection from the trailing hemisphere (equation (3)), preferential ejection from the "dark units" of Europan terrain as described above. Case 2, shown in Figure 3b, has a much closer resemblance to the observation (Figure 1) than case 1, although it is about an order of magnitude dimmer. Since the brightness (in Rayleighs) is proportional to Na density times the electron density, an increase in both quantities within the known uncertainties could account for the difference.

[21] Because the electron environment used in cases 1 and 2 was not particularly realistic, in case 3 we altered the case 2 simulation to include a latitude and longitude

Table 1. Summary of Parameters for Various Cases

Case	Na Ejection Distribution	Electron Density Distribution
1	equation (3)	uniform
2	equation (3) and preferential emission from dark regions	uniform
3	equation (3) and preferential emission from dark regions	equation (4)
4	preferential emission from dark regions	equation (4)

dependence that approximates the model of *Saur et al.* [1998]

$$\rho = 1000 + 9000 \sin(\vartheta)\mathrm{cm}^{-3}, \tag{4}$$

where ρ is the electron density and ϑ is the angle away from a specific point on the trailing hemisphere, a point on the equator, 20°E of the trailing hemisphere apex [see also *Kabin et al.*, 1999; *Paranicas et al.*, 2001]. This is unrealistic for regions near the leading hemisphere apex, where Saur et al. predicted an electron cavity, but the Cassini observations were primarily of the trailing hemisphere. In case 3 we used the same rate coefficient and vertical electron density distribution as cases 1 and 2 (exponential falloff with height proportional to surface density). Case 3 is shown in Figure 3c. Although it is quite similar to case 2, it appears to slightly better reproduce the nonuniformity seen in Figure 1. Again, the calculated brightness is an order of magnitude smaller than the observational estimate.

[22] For case 4 we used the parameters of case 3, including the electron density described by equation (4), but without including the global contribution to the dark material in equation (3). The result is shown in Figure 3d. Even without use of equation (3), preferential emission from the trailing hemisphere, which has more dark terrain, is seen. The results again approximate the Cassini observation (Figure 1), though not as well as Figures 3b and 3c.

4. Discussion

[23] We have shown that preferential ejection of Na from Europa's dark terrain, along with electron impact excitation, can produce an enhancement in auroral emission on the Jovian facing terminator on the trailing hemisphere, such as was seen by Cassini observations of Europa in eclipse. Our calculations, based in part on what is known from Earth-based observations of the Na atmosphere in sunlight, fall short of the estimated brightness by about an order of magnitude. This could be due to a combination of uncertainties in the sodium concentration in the surface, the sputtering rate, and the electron density, as well as the uncertainties in the signal discussed earlier. Since the brightness is directly proportional to electron density times Na density in the atmosphere, the latter of which is directly proportional to the Na source rate, a factor of a few in both densities would supply the needed 10 kR. This is conceivable, as the high-energy ion flux varies by up to a factor of 5 [*Paranicas et al.*, 2002], and the electron density near the surface is variable and poorly constrained [*Kliore et al.*, 1997].

[24] The dark terrain has a higher concentration of an unknown hydrated substance, some of which may be Na-containing hydrated salts [*Orlando et al.*, 2005; *Spencer et al.*, 2006]. The localized dark terrain discussed above is associated with geological features suggestive of an ocean-surface interaction [*Fanale et al.*, 1999], which might provide the surface with salts. However, the global darkness pattern of equation (3) has been associated with sulfur-ion flux, which, including the low-energy plasma, predominantly impacts the trailing hemisphere [*Pospieszalska and Johnson*, 1989]. This sulfur implantation leads to hydrated sulfuric acid, which has spectral properties similar to a Na-containing hydrated salt [*Carlson et al.*, 2005]. We distinguished between the localized and global dark terrain patterns, but although the comparison to the images is only very rough, our results suggest that sodium ejection is probably correlated with both types of dark terrain (compare Figures 1a and 1b to Figure 1c). This association between equation (3) and sodium ejection could also be due, in part, to the preferential implantation of sodium on the trailing hemisphere [*Johnson et al.*, 2000].

[25] The Cassini images show an aurora that is slightly farther north than our simulations. This could be because the spatial distribution of Na concentration used in our model is incorrect, or it could be that our electron density is greater in the northern hemisphere than in the southern hemisphere. *Leblanc et al.* [2005] included cases in which the spatial ejection distribution of Na (they used equation (3)) was shifted north or south because of the tilt in the Jovian field. However, the Cassini observations were made while Europa was near the centrifugal equator [*Porco et al.*, 2003].

[26] Our simulations examine the possible relationship between surface composition and ejection distribution. If sputtering is the dominant ejection process, then the spatial distribution of sodium ejection is likely a result of surface composition since the energetic ions that do most of the sputtering impact the surface nearly uniformly [*Paranicas et al.*, 2002]. Desorption by both the low-energy and very energetic electrons would preferentially occur on the trailing hemisphere. However, on the basis of the fluxes and the desorption cross sections [*Yakshinskiy and Madey*, 2001] this would require a large population of Na adsorbed on the surface of regolith grains. Using estimates of the sodium concentration on the trailing hemisphere [e.g., *Johnson*, 2000] and the assumption that Na is sputtered with H_2O as discussed above, a simple calculation shows that sputtering alone can produce a sodium source rate comparable to the observationally-constrained results of *Leblanc et al.* [2005].

[27] **Acknowledgments.** T.A.C. wishes to acknowledge helpful discussions with M. A. McGrath and K. Retherford. T.A.C.'s work was supported with a NASA Graduate Student Research Program fellowship through the Langley Research Center and a fellowship from the Virginia Space Grant Consortium. R.E.J. acknowledges support from NASA's Planetary Atmospheres and Planetary Geology and Geophysics Programs.

References

Ajello, J. M., G. K. James, and I. Kanik (1992), The complete UV spectrum of SO_2 by electron impact: 2. The middle ultraviolet spectrum, *J. Geophys. Res.*, *97*, 10,501–10,512.

Allen, J. S., L. W. Anderson, and C. L. Chun (1988), Cross sections for excitation of Na by impact of H^+, H_2^+, H_3^+, and H^- ions, *Phys. Rev. A*, *37*, 349–355.

Brown, M. E. (2001), Potassium in Europa's atmosphere, *Icarus*, *151*, 190–195.
Burger, M. H., and R. E. Johnson (2004), Europa's neutral cloud: Morphology and comparisons to Io, *Icarus*, *171*, 557–560.
Carlson, R. W., M. S. Anderson, R. Mehlman, and R. E. Johnson (2005), Distribution of hydrate on Europa: Further evidence for sulfuric acid hydrate, *Icarus*, *177*, 461–471.
Cassidy, T. A., and R. E. Johnson (2005), Monte Carlo model of sputtering and other ejection processes within a regolith, *Icarus*, *176*, 499–507.
Cassidy, T. A., R. E. Johnson, M. A. McGrath, M. C. Wong, and J. F. Cooper (2007), The spatial morphology of Europa's near-surface O_2 atmosphere, *Icarus*, *191*, 755–764.
Fanale, F. P., et al. (1999), Galileo's multiinstrument spectral view of Europa's surface composition, *Icarus*, *139*, 179–188.
Geissler, P., A. McEwen, C. Porco, D. Strobel, J. Saur, J. Ajello, and R. West (2004), Cassini observations of Io's visible aurorae, *Icarus*, *172*, 127–140.
Hall, D. T., P. D. Feldman, M. A. McGrath, and D. F. Strobel (1998), The far-ultraviolet oxygen airglow of Europa and Ganymede, *Astrophys. J.*, *499*, 475–481.
Johnson, R. E. (2000), Sodium at Europa, *Icarus*, *143*, 429–433.
Johnson, R. E., F. Leblanc, B. V. Yakshinskiy, and T. E. Madey (2002), Energy distributions for desorption of sodium and potassium from ice: The Na/K ratio at Europa, *Icarus*, *156*, 136–142.
Johnson, R. E., R. W. Carlson, J. F. Cooper, C. Paranicas, M. H. Moore, and M. C. Wong (2004), Radiation effects on the surfaces of the Galilean satellites, in *Jupiter: The Planet, Satellites, and Magnetosphere*, edited by F. Bagenal et al., pp. 485–512, Cambridge Univ. Press, Cambridge, U. K.
Kabin, K., M. R. Combi, T. I. Gombosi, A. F. Nagy, D. L. DeZeeuw, and K. G. Powell (1999), On Europa's magnetospheric interaction: A MHD simulation of the E4 flyby, *J. Geophys. Res.*, *104*, 19,983–19,992.
Kanik, I., C. Noren, O. P. Makarov, P. Vattipalle, J. M. Ajello, and D. E. Shemansky (2003), Electron impact dissociative excitation of O_2: 2. Absolute emission cross sections of the OI(130.4 nm) and OI(135.6 nm) lines, *J. Geophys. Res.*, *108*(E11), 5126, doi:10.1029/2000JE001423.
Kim, Y. (2001), Scaling of plane-wave born cross sections for electron-impact excitation of neutral atoms, *Phys. Rev. A*, *64*, 032714, doi:10.1103/PhysRevA.64.032714.
Kliore, A. J., D. P. Hinson, F. M. Flasar, A. F. Nagy, and T. E. Cravens (1997), The ionosphere of Europa from Galileo radio occultations, *Science*, *277*, 355–358.
Leblanc, F., R. E. Johnson, and M. E. Brown (2002), Europa's sodium atmosphere: An ocean source?, *Icarus*, *159*, 132–144.
Leblanc, F., A. E. Potter, R. M. Killen, and R. E. Johnson (2005), Origins of Europa Na cloud and torus, *Icarus*, *178*, 367–385.
McEwen, A. S. (1986), Exogenic and endogenic albedo and color patterns on Europa, *J. Geophys. Res.*, *91*, 8077–8097.
McGrath, M. A., E. Lellouch, D. F. Strobel, P. D. Feldman, and R. E. Johnson (2004), Satellite atmospheres, in *Jupiter: The Planet, Satellites, and Magnetosphere*, edited by F. Bagenal et al., pp. 457–483, Cambridge Univ. Press, Cambridge, U. K.
Orlando, T. M., T. B. McCord, and G. A. Grieves (2005), The chemical nature of Europa surface material and the relation to a subsurface ocean, *Icarus*, *177*, 528–533.
Paranicas, C., R. W. Carlson, and R. E. Johnson (2001), Electron bombardment of Europa, *Geophys. Res. Lett.*, *28*, 673–676.
Paranicas, C., J. M. Ratliff, B. H. Mauk, C. Cohen, and R. E. Johnson (2002), The ion environment near Europa and its role in surface energetics, *Geophys. Res. Lett.*, *29*(5), 1074, doi:10.1029/2001GL014127.
Porco, C. C., et al. (2003), Cassini imaging of Jupiter's atmosphere, satellites, and rings, *Science*, *299*, 1541–1547.
Porco, C. C., et al. (2004), Cassini imaging science: Instrument characteristics and anticipated scientific investigations at saturn, *Space Sci. Rev.*, *115*, 363–497.
Pospieszalska, M. K., and R. E. Johnson (1989), Magnetospheric ion bombardment profiles of satellites: Europa and Dione, *Icarus*, *78*, 1–13.
Reimann, C. T., J. W. Boring, R. E. Johnson, L. W. Garrett, and K. R. Farmer (1984), Ion-induced molecular ejection from D_2O ice, *Surf. Sci.*, *147*, 227–240.
Saur, J., D. F. Strobel, and F. M. Neubauer (1998), Interaction of the Jovian magnetosphere with Europa: Constraints on the neutral atmosphere, *J. Geophys. Res.*, *103*, 19,947–19,962.
Smyth, W. H., and M. L. Marconi (2000), Io's oxygen source: Determination from ground-based observations and implications for the plasma, *J. Geophys. Res.*, *105*, 7783–7792.
Smyth, W. H., and M. L. Marconi (2006), Europa's atmosphere, gas tori, and magnetospheric implications, *Icarus*, *181*, 510–526.
Spencer, J., W. Grundy, C. Dumas, R. W. Carlson, T. B. McCord, G. B. Hansen, and R. J. Terrile (2006), The nature of Europa's dark non-ice surface material: Spatially-resolved high spectral resolution spectroscopy from the Keck telescope, *Icarus*, *182*, 202–210.
Wiens, R. C., D. S. Burnett, W. F. Calaway, C. S. Hansen, K. R. Lykke, and M. J. Pellin (1997), Sputtering products of sodium sulfate: Implications for Io's surface and for sodium-bearing molecules in the Io torus, *Icarus*, *128*, 386–397.
Yakshinskiy, B. V., and T. E. Madey (2001), Electron- and photon-stimulated desorption of K from ice surfaces, *J. Geophys. Res.*, *106*, 33,303–33,307.
Zipf, E. C., R. W. McLaughlin, and M. R. Gorman (1978), A study of the excitation and radiative decay of the $3s'^3D^o$ and $3d^3D^o$ levels of atomic oxygen, *Planet. Space Sci.*, *27*, 719–732.
Zolotov, M. Y., and E. L. Shock (2001), Composition and stability of salts on the surface of Europa and their oceanic origin, *J. Geophys. Res.*, *106*, 32,815–32,827.

T. A. Cassidy and R. E. Johnson, Engineering Physics Program and Department of Astronomy, University of Virginia, P.O. Box 400325, Charlottesville, VA 22904-4325, USA.
P. E. Geissler, U.S. Geological Survey, 2255 North Gemini Drive, Flagstaff, AZ 86001, USA.
F. Leblanc, Service d'Aéronomie du CNRS, Reduit de Verrieres -BP 3, Verrières-le-Buisson, F-91371, France.